

AD-A236 247



OFFICE OF NAVAL RESEARCH

Contract N00014-89-J-1028

Technical Report No. 10

Photodegradation of Polyimides. V.  
An Explanation of the Rapid Photolytic Decomposition of a Selected  
Polyimide via Anhydride Formation

by

C.E. Hoyle<sup>1</sup>, E.T. Anzures<sup>1</sup>, P. Subramanian<sup>2</sup>,  
R. Nagarajan<sup>1</sup>, and D. Creed<sup>2</sup>

Prepared for Publication in

Macromolecules

<sup>1</sup>Department of Polymer Science  
University Southern Mississippi  
Hattiesburg, MS 39406-0076

<sup>2</sup>Department of Chemistry and Biochemistry  
University of Southern Mississippi  
Hattiesburg, MS 39406-5043



Classification For	
DTIC	<input checked="" type="checkbox"/>
DTIC Tab	<input type="checkbox"/>
DTIC Hood	<input type="checkbox"/>
Classification	
By	
Date	
DTIC Tab	
DTIC Hood	
Classification	
A-1	

Reproduction in whole or in part is permitted for any purpose of the United States government.

This document has been approved for public release and sale: its distribution is unlimited.

91 6 4 080

91-01195

REPORT DOCUMENTATION PAGE

1a. REPORT SECURITY CLASSIFICATION NONE		1b. RESTRICTIVE MARKINGS NONE	
2a. SECURITY CLASSIFICATION AUTHORITY NONE		3. DISTRIBUTION / AVAILABILITY OF REPORT UNLIMITED	
2b. DECLASSIFICATION / DOWNGRADING SCHEDULE NONE			
4. PERFORMING ORGANIZATION REPORT NUMBER(S) Technical Report No. 10		5. MONITORING ORGANIZATION REPORT NUMBER(S) ONR N0014-89-J-1028	
6a. NAME OF PERFORMING ORGANIZATION University of Southern Mississippi	6b. OFFICE SYMBOL (if applicable)	7a. NAME OF MONITORING ORGANIZATION Office of Naval Research	
6c. ADDRESS (City, State, and ZIP Code) University of Southern Mississippi Polymer Science Department Southern Station Box 10076 Hattiesburg, MS 39406-0076		7b. ADDRESS (City, State, and ZIP Code) 800 North Quincy Avenue Arlington, VA 22217	
8a. NAME OF FUNDING / SPONSORING ORGANIZATION Office of Naval Research	8b. OFFICE SYMBOL (if applicable)	9. PROCUREMENT INSTRUMENT IDENTIFICATION NUMBER	
8c. ADDRESS (City, State, and ZIP Code) 800 N. Quincy Avenue Arlington, VA 22217		10. SOURCE OF FUNDING NUMBERS	
		PROGRAM ELEMENT NO.	PROJECT NO.
		TASK NO.	WORK UNIT ACCESSION NO.
11. TITLE (Include Security Classification) Photodegradation of Polyimides. V. An Explanation of the Rapid Photolytic Decomposition of a Selected Polyimide via Anhydride Formation			
12. PERSONAL AUTHOR(S) C.E. Hoyle, E.T. Anzures, P. Subramanian			
13a. TYPE OF REPORT Technical	13b. TIME COVERED FROM 6-1-90 TO 5-31-91	14. DATE OF REPORT (Year, Month, Day) 91-05-31	15. PAGE COUNT
16. SUPPLEMENTARY NOTATION			
17. COSATI CODES		18. SUBJECT TERMS (Continue on reverse if necessary and identify by block number)	
FIELD	GROUP	SUB-GROUP	
19. ABSTRACT (Continue on reverse if necessary and identify by block number) <p>The photolytic decomposition in air of a polyimide film based on a dianhydride and a diarylamine with hexafluoroisopropylidene 6F bridging groups is extremely rapid leading to efficient chain cleavage and subsequent photooxidative decomposition. Relatively short photolysis times with an unfiltered medium pressure mercury lamp are required to give a clean photoablation process of the 6F-6F polyimide films in air. IR difference spectroscopy shows the appearance of anhydride groups on photolysis in air indicating a photooxidation process via decomposition of the arylimide linkage. A photophysical and photochemical analysis of several model N-arylphthalimides indicates that both solvent polarity and electron withdrawing/donating substituents can greatly alter the efficiency of the photolysis process. The formation of the triplet state is also dependent on the substituents and solvent.</p>			
20. DISTRIBUTION / AVAILABILITY OF ABSTRACT <input checked="" type="checkbox"/> UNCLASSIFIED/UNLIMITED <input checked="" type="checkbox"/> SAME AS RPT. <input type="checkbox"/> DTIC USERS		21. ABSTRACT SECURITY CLASSIFICATION	
22a. NAME OF RESPONSIBLE INDIVIDUAL Ken Wynne		22b. TELEPHONE (Include Area Code) (601)266-4868	22c. OFFICE SYMBOL

Photodegradation of Polyimides. V. An Explanation of the Rapid  
Photolytic Decomposition of a Selected Polyimide  
via Anhydride Formation

by

C.E. Hoyle<sup>1</sup>, E.T. Anzures<sup>1</sup>, P. Subramaniam<sup>2</sup>,  
R. Nagarajan<sup>1</sup>, and D. Creed<sup>2</sup>

<sup>1</sup>Department of Polymer Science  
University of Southern Mississippi  
Hattiesburg, MS 39406-0076

<sup>2</sup>Department of Chemistry and Biochemistry  
University of Southern Mississippi  
Hattiesburg, MS 39406-5043

**ABSTRACT**

The photolytic decomposition in air of a polyimide film based on a dianhydride and a diarylamine with hexafluoroisopropylidene 6F bridging groups is extremely rapid leading to efficient chain cleavage and subsequent photooxidative decomposition. Only relatively short photolysis times with an unfiltered medium pressure mercury lamp are required to give a clean photoablation process of the 6F-6F polyimide films in air. IR difference spectroscopy shows the appearance of anhydride groups on photolysis in air indicating a photooxidation process via decomposition of the arylimide linkage. A photophysical and photochemical analysis of several model N-arylphthalimides indicates that both solvent polarity and electron withdrawing/donating substituents can greatly alter the efficiency of the photolysis process. The formation of the triplet state is also dependent on the substituents and solvent polarity.

91 6 4 082

91-01198  


## INTRODUCTION

In a recent series of papers, we reported the result of an extensive investigation of the photodegradation of aryl polyimides (1-5). The polyimides studied were based on a variety of dianhydrides (shown below) with oxydianiline (ODA) and methylenedianiline (MDA). In all of the polyimides investigated in our laboratory to date, work has focused on the effect of a bridging group such as carbonyl, oxygen, or hexafluoroisopropylidene on the inherent photostability of the polyimide structure (1-5). In general we find that replacement of the pyromellitic dianhydride (PMDA) used to generate, along with oxydianiline (ODA), the PMDA-ODA polyimides [which are the basis of the high temperature resistant arylimide films known as Kapton™ (DuPont)] with the 6F dianhydride leads to a lowering of resistance to light exposure from the unfiltered output of a medium pressure mercury lamp. The photooxidative stability of the PMDA-ODA polyimide film may be related in part to the charge transfer nature of the excited state as well as the effect of the pyromellitimide moiety on the stability of reactive intermediates formed. Since the pyromellitimide group is a strong electron acceptor, it is not unreasonable to suspect that the strong charge transfer excited state formed would indeed alter both the radiative and non-radiative reactivities of the excited state. The absorption and fluorescence bands are certainly influenced markedly by the high degree of charge transfer afforded by the pyromellitimide group (6-12).

In the present paper, we focus attention on the nature of the electron donor properties of the diamine portion of the polyimide. We find that by altering the substituents on the aryl moiety of N-aryl phthalimides, both photophysical properties such

as absorption and emission maxima, triplet yields, and chemical properties, such as photoproduct formation, are greatly altered. The effect of electron donating and electron withdrawing bridging groups on the diamine part of a hexafluoroisopropylidene (6F) dianilinyli dianhydride based polyimide will be discussed with respect to the ultimate photolability of the polymer film.

## EXPERIMENTAL

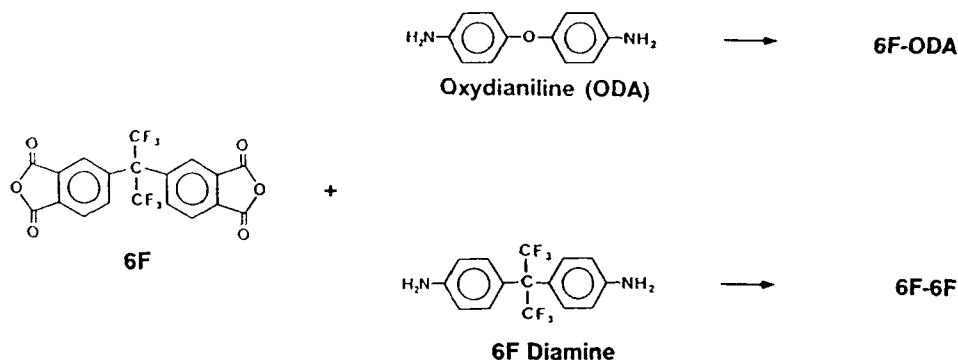
All solvents were obtained from Burdick and Jackson and used as received. Model compounds were synthesized by a procedure analogous to that described in the previous paper in this series (5). Elemental analysis performed by Galbraith Laboratories was in excellent agreement for each model compound. The polyimide synthesis and film preparation have already been described thoroughly (1-5). Polymer film photolysis was conducted with a 450 W Canrad Hanovia medium pressure mercury lamp in air or nitrogen, as appropriate. Gel permeation chromatography was performed for all polymers with a THF mobile phase on a Waters system using 100, 500,  $10^4$ , and  $10^5$  columns. All molecular weights are reported relative to polystyrene standards. For model compound quantum yield measurements, band pass filters were used to isolate a specific line from a medium pressure mercury lamp. Samples were irradiated in a 1-cm pathlength cell, and the light intensities determined by ferrioxalate actinometry. Product formation was followed by comparison of gas chromatography retention times with those of authentic samples. Details are given in the previous paper in this series (5).

A Perkin-Elmer 1600 Fourier transform infrared (FT-IR) spectrometer was used for recording infrared spectra. UV spectra were obtained on a Perkin-Elmer Lambda 6 UV-VIS spectrophotometer. Fluorescence spectra were obtained on a Spex Fluorolog-2 with 1.5 mm slits.

The laser flash photolysis experiments were carried out in a unit consisting of a Lumonics HyperEx 440 excimer laser excitation source and an Applied Photophysics Xenon lamp/monochromator/PMT monitoring system. The signal from the PMT is sent to a Phillips model PM 3323 programmable digital oscilloscope. Data is transferred from the oscilloscope to an Archimedes desktop computer (Acorn Computers Ltd., U.K.) via the IEEE-488 instrument interface bus, which also sends control to the digital oscilloscope and LASER software package. The xenon lamp monitoring source (right-angle arrangement) was momentarily pulsed to achieve a high intensity monitoring beam that was of near constant intensity for about 200  $\mu$ s. The laser was operated at 248 nm ( $\text{KrF}^+$ ). Nominal outputs were 80 mJ/pulse at 248 nm. In the laser flash photolysis experiments, all samples were contained in a 1 cm x 1 cm x 4 cm quartz fluorescence cell. In order to ensure oxygen-free samples, solutions were bubbled with nitrogen prior to the experiment. All the solutions had absorbances of approximately 1.0 at 248 nm. The data analysis system is a complete data acquisition and analysis system for the Applied Photophysics LKS.50 Laser Flash Photolysis Spectrometer. Time resolved absorption spectra of transient intermediates were compiled from the individual wavelength encoded kinetic data files using Applied Photophysics software.

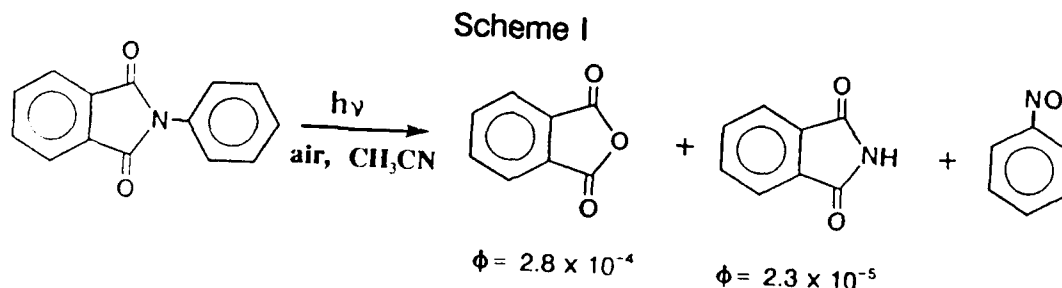
## RESULTS AND DISCUSSION

The results will be presented in three parts. In the first part, we consider the effect of substituents in the para position of N-aryl phthalimides on the resulting photochemistry and photophysics in oxygen saturated solutions. In addition, the spectroscopic and photolytic consequences of the polarity of the solvent on the photolysis process of N-phenylphthalimide (PA-A) are presented. Based on these results, the rapid photolytic degradation of polyimide films made from the hexafluoroisopropylidene containing dianhydride (6F dianhydride) shown below and two dianilines with oxygen and hexafluoroisopropylidene (6F diamine) bridging groups (see structures and the appropriate designations for the polymers) are interpreted.



### Photophysics and Photochemistry of N-arylphthalimides

In a previous report, we showed that photolysis of N-phenylphthalimide (designated PA-A) in an air saturated acetonitrile solution resulted in the formation of phthalic anhydride and phthalimide as identifiable primary photoproducts (Scheme I) in a ratio of about 10:1.



Although we could not obtain absolute identification, we have circumstantial evidence for the formation of nitrosobenzene as a primary product: nitrobenzene was identified and probably forms from the efficient photooxidation of nitrosobenzene. As indicated in Scheme I, the quantum yields for product formation in air saturated acetonitrile are relatively low. However, they are reasonable values when compared to the extremely low yields for product formation of bis N-arylpyromellitimides: the quantum yield for disappearance of bisphenylpyromellitimide is estimated to have a lower value in acetonitrile. The stability of the pyromellitimide may result, in part, from the significant charge transfer character of the excited states. PA-A thus serves as a reasonable model for the repeat unit in 6F-ODA which does not possess as strong an electron acceptor as the pyromellitimide group of PMDA-ODA polyimides.

We know that increasing the electron accepting ability of the dianhydride based portion of the imide repeat unit results in increased photostability of the polymer as well as a shift in the charge transfer absorption band to the red accompanied by an increase in the energy of charge transfer emission. We might expect that altering the electron donating ability of the aromatic diamine based portion of the polyimide repeat unit might well result in changes in spectroscopic (*absorption, emission*) and photochemical properties of the repeat unit. We might also expect that any changes in the polarity of the environment (eg. a solvent) in which the polyimide repeat unit, or an appropriate model compound, is located should also alter the spectroscopic and photochemical properties. Thus, by exploring the effect of the electron donating ability of the N-aryl

groups and the effect of solvent polarity, it should be possible to better define factors which lead to photoreactivity in the polyimide.

We begin by exploring the effect of solvents on the absorption and fluorescence spectra of N-phenylphthalimide (PA-A). Figure 1 shows the absorption spectra of PA-A in acetonitrile ( $\epsilon = 37.7$ ), dichloromethane ( $\epsilon = 9.08$ ), and cyclohexane ( $\epsilon = 2.023$ ) above 260 nm. Two features of these spectra are worthy of note. There is a structured band at higher energies and absorption tailing above 350 nm. The absorption characteristics of PA-A and its response to solvent polarity is probably complicated involving both conventional transitions and charge transfer states, all of which are subject to solvents effects. Evidence for a charge-transfer (CT) excited state in PA-A comes from the broad structureless fluorescence of PA-A (Figure 2) that is red shifted from 490 to 525 to 535 nm as the solvent becomes more polar in changing from cyclohexane to dichloromethane to acetonitrile. The large Stokes shift between the absorption and emission spectra suggests this CT state has a geometry quite different from that of the vertical or Franck Condon state formed at the instant of excitation. This relaxed CT state may be a twisted intramolecular CT state of the type proposed for N,N-dimethylaminobenzonitrile (13) and suggested by Frank (11) to perhaps be partly responsible for the fluorescence of polyimides. In addition to being red shifted, this fluorescence becomes much weaker in acetonitrile presumably because it is increasingly solvent stabilized. Its energy is lowered and non-radiative decay competes more effectively with fluorescence.

In considering rate processes affected by the solvent polarity, the intersystem crossing from the singlet to the triplet excited state should be considered. Figure 3

shows the transient absorption spectra of PA-A in nitrogen (Figure 3a) and air (Figure 3b) saturated acetonitrile solutions. The transient spectra in nitrogen are characterized by two higher energy peak maxima at approximately 300 nm and 330 nm and a broad absorption band centered around 500 nm. Decay constants obtained by fitting the decay of the transient spectra to a single exponential decay function are about  $8.5 \times 10^4 \text{ sec}^{-1}$  at wavelengths from 300 nm to 500 nm for a nitrogen saturated PA-A solution. All of the structural features decay with approximately the same exponential rate constant, i.e., all have a lifetime of approximately 11.5  $\mu\text{sec}$ . This is quite consistent with decay of a single transient species with strong absorption at 300-330 nm and weaker absorption at 470-530 nm.

In attempting to identify the transient species responsible for the absorption bands in Figure 3, we first note that oxygen effectively quenches all of the structural features uniformly (Figure 3b). This suggests that the transient arises from either a radical species which is efficiently quenched by oxygen, or a triplet state. Addition of low concentrations of cyclohexadiene ( $1 \times 10^{-4} \text{ M}$  or less) results in the uniform lifetime quenching of all transient peaks in a nitrogen saturated acetonitrile solution of PA-A. Figure 4 shows a Stern-Volmer plot of the ratio of the transient lifetime before and after adding quencher as a function of the cyclohexadiene concentration. The quenching rate constant of  $6.0 \times 10^9 \text{ l mole}^{-1} \text{ sec}^{-1}$  calculated from the slope is essentially diffusion controlled. This is expected for quenching of a triplet state by cyclohexadiene, which has a triplet with energy of only 54 kcal. If the transient spectra resulted from a radical or biradical species, a diffusion, or near diffusion, controlled quenching rate would certainly not be

expected. Results of both oxygen and cyclohexadiene quenching experiments suggest that the transient spectra in Figure 3 are due to a triplet intermediate with a lifetime of 11.5  $\mu$ sec. Additional work to confirm this premise will be published in a separate mechanistic paper.

Figures 5 and 6 show the transient absorption spectra of PA-A in dichloromethane and cyclohexane. If the absorbances at the maxima are taken as representing the relative triplet yields, then the amount of triplet generated in cyclohexane is much greater than in dichloromethane or acetonitrile (Table 1). This result nicely parallels the red shifts and reductions in intensity of fluorescence observed (Figure 2) in going from cyclohexane to the two more polar solvents. Presumably, solvent stabilization of the relaxed CT state accelerates non-radiative decay processes thereby reducing the probability of intersystem crossing to the triplet as well as the probability of fluorescence.

Based on the spectroscopic/transient observations in Figures 1-6, we would expect that the polarity of the solvent might have a significant effect on the photochemical processes. Photolysis of PA-A was therefore conducted with the isolated 313 nm line (band pass filter used to isolate line) of a medium pressure mercury lamp. The light intensity was measured with ferrioxalate actinometry and the product yields and loss of reactant determined by gas chromatographic analysis of the photolyzed samples in different solvents. The quantum yields for disappearance,  $\Phi_{\text{loss}}$ , and the quantum yield for phthalic anhydride formation, ( $\Phi_{\text{PhAnh}}$ ) in air saturated solutions are given in Table I for direct comparison with fluorescence emission maxima and relative transient (triplet state) yields. Only results for the primary photooxidation product quantum yield are given. The

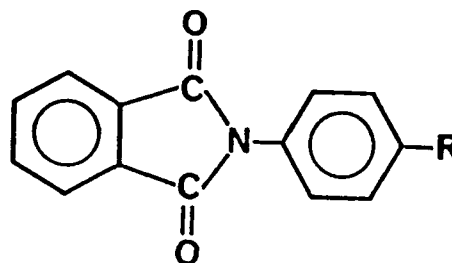
most noticeable result is that the red shift in the fluorescence emission maxima and the increase in relative transient triplet yield is accompanied by an increase in product quantum yield and disappearance yield in cyclohexane, a non-polar solvent. Since the major products formed in cyclohexane are identical to those in acetonitrile, no significant alteration in the mechanism for decomposition is indicated. The high quantum yield for reactant loss in cyclohexane accompanies an expected decrease in the non-radiative rate constant of the charge-transfer excited state in the non-polar cyclohexane solvent and a shift of the fluorescence maximum to higher energies.

At this juncture in our discussion it is worth considering the effect of solvent on the relative population of excited states. At 313 nm, the wavelength of excitation in the quantum yield experiments, there is the possibility of absorbance due to a number of conventional transitions as well as a charge transfer transition. The solvent polarity may well alter the absorbing states at the 313 nm excitation wavelength, as well as the related excited state energy and the processes occurring from the relaxed state or states. For purposes of this paper, we simply note that the solvent alters the quantum efficiency of the photooxidation process significantly. Differentiation between and quantitation of the various factors which solvent polarity can affect, as well the spin multiplicity of the precursor excited state leading to product formation will be covered in a separate paper. Since multiple states are involved in the absorption process, the possibility of wavelength dependent photochemistry is possible and will be considered in a future study.

Having established the effect of solvent polarity, and the resultant blue shift in the emission wavelength which is accompanied by increased triplet formation and product

yield, we investigated the effect of para substituents on the spectroscopic/photochemical properties of N-phenylphthalimide (see structures and appropriate designations) with a view to exploring substituent effects on the charge-transfer state.

R	Designation
H	PA-A
OPh	PA-POA
CN	PA-CNA
Cl	PA-CIA



The absorption and emission spectra are given in Figures 7 and 8. The absorption spectra are complex and difficult to interpret although the quite different absorption spectrum of PA-POA is almost certainly due to the additional conjugation afforded by the phenoxyaryl moiety. The fluorescence maxima (Table II) leave no doubt that the relaxed CT state is stabilized by electron donating groups (eg. PhO-) on the N-aryl group and destabilized by electron withdrawing groups (eg. CN) in the same position. Thus, the phenoxy substituent shifts the emission to the red of that of PA-A (the emission also becomes very weak) and the cyano group shifts it to the blue. The N-aryl group, not surprisingly, is the donor component in the CT state! The effect of reducing CT stabilization by changing the N-aryl substituent from PhO to H to CN roughly parallels the effect of reducing solvation of the CT state by changing the solvent for PA-A fluorescence from acetonitrile to dichloromethane to cyclohexane.

The disappearance quantum yields ( $\Phi_{\text{loss}}$ ) and quantum yields for phthalic anhydride formation ( $\Phi_{\text{PhAnh}}$ ) upon photolysis at 313 nm are also given in Table II.

Substitution of the phenoxy group results in a decrease in the disappearance quantum yield by about one order of magnitude, while the electron withdrawing cyano group has the opposite effect. In addition, the relative transient quantum yields in acetonitrile (presumably the triplet yields) in Table II also show a large increase for the cyano group paralleling the increased starting material disappearance and product formation quantum yields and the shift in the fluorescence maximum to higher energies. Again, the substitution of electron withdrawing groups at a para position appears to have the same effect as decreasing solvent polarity on both triplet and product yields. Apparently the substitution of electron withdrawing substituents on the N-phenyl ring results in a decrease in the electron donor properties of the phenyl group and a concomitant higher energy charge transfer state, i.e, there is less charge-transfer character in the excited state. The large difference in product quantum between PA-POA and PA-CNA is dramatic: about two orders of magnitude! Thus, the effect of electron donating/withdrawing groups and their role in the excited state photochemistry, as well as any effect they have on subsequent dark reactions, must be taken into account in the photooxidation of polyimides. Since the initial reaction of the primary process of the N-arylphthalimides may be an  $\alpha$ -cleavage of the N-CO band to give a diradical which can react with oxygen (5), the rate of diradical ring closure versus interception by oxygen could well be affected by the substituents.

## Photolysis of Polyimide Films Based on 6F Dianhydride

Since it has been established in the small molecule photolysis investigation that the electron donating/withdrawing effect of groups substituted at the para position in N-phenyl phthalimides can alter the photochemical and spectroscopic properties by a significant degree, it is reasonable to speculate that the chemical structure of the diamine moiety might have a profound effect on the resultant photochemistry of polyimide films. In a recent series of papers, we already reported that any structural feature which alters the electron accepting ability of the dianhydride based chromophore, i.e., termed the acceptor, can markedly alter the photodecomposition of the polyimide film (1-4). For example, replacement of the typical pyromellitic dianhydride by the 6F dianhydride results in a dramatic decrease in the photooxidative stability of the resultant polyimide film. Model compound studies indicate that the more stable pyromellitimide repeat unit is characterized by a more well defined charge transfer state. Since in the present paper, model compound studies indicate that the photooxidation of N-phenyl phthalimide is enhanced by a para electron withdrawing group, we chose to investigate the photolysis of polyimide films derived from the same 6F dianhydride repeat unit, but with diamines based on oxydianiline (ODA) and the 6F diamine, i.e., the 6F-ODA and 6F-6F polyimides. Since the bridging hexafluoroisopropylidene moiety is probably a very good electron withdrawing (group), one might expect that the 6F-6F polyimide films would be even more unstable than the 6F-ODA polyimide films which themselves have already been shown to

be photooxidatively unstable (relative to PMDA-ODA films) when exposed to the unfiltered output of a medium pressure mercury lamp in air.

Figure 9 shows comparative absorption spectra of thin 6F-6F, 6F-ODA, and PMDA-ODA films. The shift to the blue of the tail of the charge transfer absorption band occurs in the order 6F-6F, 6F-ODA, PMDA-ODA. If we based a prediction of the photooxidative rate of the three polyimide films strictly on the intensity of the absorption bands, we might speculate that for a given film thickness the PMDA-ODA film would degrade at a faster rate than 6F-ODA and 6F-6F films since it has a higher absorbance at a given wavelength. However, Figure 10 shows FT-IR spectra of the 6F-ODA and 6F-6F films at 12 and 3 hours photolysis times, respectively, with an unfiltered medium pressure mercury lamp. After only 3 hours, the 6F-6F film shows decreases in most bands. After greater than four hours of exposure the 6F-6F films are essentially decomposed and reliable IR spectra cannot be obtained. The 6F-ODA films show similar losses in all absorbance bands but for a longer photolysis time. Clearly the 6F-6F films are being photooxidized at a very high rate. Incidentally, photolysis of 6F-6F or 6F-ODA films in a nitrogen atmosphere leads to almost no degradation even for very long exposure times, thus indicating that a photooxidative process is operative as discussed in previous papers (4, 5). The GPC chromatograms in Figure 12 of photolyzed 6F-6F films (initial molecular weight at peak maximum of 56,700 compared to polystyrene standards) indicate an extremely rapid loss in molecular weight after photolysis times of only 1 hour. Comparison with similar data for 6F-ODA films in Figure 13, which plots peak molecular weight versus photolysis time, shows that 6F-6F films are degraded to extremely low molecular weights in times much

less than 5 hours. In fact, as indicated already, photolysis for times longer than 4 hours results in 6F-6F films which are severely decomposed and experience large weight losses. Although this also eventually happens for 6F-ODA films, it takes well over 20 hours exposure to the same unfiltered light source to achieve a comparable degree of decomposition and weight loss.

As indicated previously for 6F-ODA, the loss of molecular weight and film weight are both the result of efficient photooxidation processes, the latter (weight loss) requiring photolysis with wavelengths of light less than 300 nm for maximum efficiency. The GPC peak maxima results in Figure 14 demonstrate that even upon photolysis times of up to 96 hours in nitrogen, no detectable molecular weight changes are recorded. This is in accordance with the IR results in Figure 11. The photooxidative degradation process has been postulated, based on the model compounds, to proceed via a primary photooxidation step yielding phthalic anhydride as a primary product in the initial photolysis step of 6F dianhydride based polyimides. Certainly, as demonstrated in an earlier section dealing with the model compounds, as well as the previous paper in this series (5), the generation of anhydride groups upon photolysis of 6F (as well as other) dianhydride based polyimides is a viable mechanism for the initiation of the series of photochemical events that eventually lead to the ultimate ablative decomposition of the polyimide film. Indeed, as for the 6F-ODA films (4), FT-IR analysis of a gas cell of the collected products produced by the photoablation of 6F-6F films indicates that extensive amounts of carbon monoxide, carbon dioxide, and water are produced in addition to some small molecule fluorinated (probably  $\text{CF}_3\text{H}$ ) compounds.

One question which yet remains, at least from our previous work, is the lack of evidence for anhydride formation in the actual polyimide film photolysis. As reported in earlier (1), and as can be seen in Figure 10b, the photooxidation of 6F-ODA films results in an "ablation" of the film and uniform decrease in all of the IR absorption bands. No evidence for any functional groups, such as anhydrides, is observed for the photolyzed 6F-ODA films. And yet, the model compound studies of N-phenyl phthalimides indicate phthalic anhydride as the major photoproduct in air. In addition, a preliminary investigation of the model diimide made from the 6F dianhydride and aniline indicates that photolysis in an air saturated solution yields the 6F dianhydride (the identification of other products formed, as well as quantitative measurements, has not been performed). A quite simple explanation for the lack of observation of any anhydride absorbance in the IR of photolyzed 6F-ODA films, which incidentally should appear at  $1850\text{ cm}^{-1}$ ,  $1780\text{ cm}^{-1}$ , and  $900\text{ cm}^{-1}$ , follows from consideration of the relative efficiencies of the processes involved. Based on the model compound studies in solution, we know that the quantum yields for loss of N-phenyl phthalimide ( $R=H$ ) and N-para-phenoxyphenyl phthalimide ( $R=OPh$ ), which can be considered as models for the 6F-ODA repeat unit, are  $8.2 \times 10^{-4}$  and  $8.8 \times 10^{-5}$  in air saturated dichloromethane. As shown in the previous section, the exact quantum efficiencies will vary with the solvent polarity, which in the solid polyimide film might be quite different from dichloromethane. Furthermore, the two models are not exact replicas of the repeat unit. However, the quantum yields are probably a reasonable indication of the relative photolability of the imide repeat unit in the 6F-ODA film. Neglecting for a moment the phthalimide type product, which one might expect would be

very difficult to differentiate in the IR from the parent N-arylphthalimide group, we consider the relative stability of phthalic anhydride groups subjected to the same photolysis conditions, namely an unfiltered mercury lamp in an air saturated environment. The quantum efficiency for photolysis of phthalic anhydride in air saturated dichloromethane at 280 nm (it has no appreciable absorbance at 313 nm where the quantum yields for the model N-aryl phthalimides were determined) is  $5.3 \times 10^{-2}$ . This is essentially two orders of magnitude greater than the quantum yield for its formation from N-phenyl phthalimide (PA-A) and three orders of magnitude greater than its formation from N-phenoxyphenyl phthalimide. If these values are representative of the respective efficiencies in the film, then for 6F-ODA we would expect that any phthalic anhydride groups formed would be immediately photolyzed in the presence of oxygen and thus observation in the IR would be impossible. In other words, for 6F-ODA, and certainly the other polyimides studied to date, the rate determining step in the photooxidation process is the formation of phthalic anhydride moieties: the phthalic anhydride end groups would be rapidly consumed by photooxidation at a much faster rate than their formation.

As can be seen by a comparison of the IR spectra of the photolyzed film (Figure 10a) there is a new peak for the photolyzed 6F-6F film (spectrum a) at  $1853 \text{ cm}^{-1}$ . In addition, the absorbances near  $1770 \text{ cm}^{-1}$  and  $900 \text{ cm}^{-1}$  have actually increased. Figure 15 shows the difference spectrum of 6F-6F before and after 3 hours photolysis with an unfiltered lamp. The spectrum in Figure 15 was generated by subtraction of the photolyzed spectrum from the unphotolyzed spectrum. The only peaks which increase are at  $1853 \text{ cm}^{-1}$ ,  $1770 \text{ cm}^{-1}$ , and  $900 \text{ cm}^{-1}$ , all characteristic of the phthalic anhydride

moiety. All other peaks show distinct losses. The appearance of anhydride end groups is obvious for the 6F-6F polyimide. By contrast, a difference spectrum (not shown) for 6F-ODA shows loss of all structural features in the IR bands: no new bands appear.

The results for the 6F-6F film in Figure 15 are quite reasonable if account is taken of the electron withdrawing nature of the hexafluoroisopropylidene moiety. From the UV absorption spectra in Figure 1 the 6F-6F polymer can be characterized as having a high energy charge transfer state. If we consider the 6F bridging unit in the 6F-diamine to be an electron withdrawing group (Table II), we can speculate that the rate of anhydride formation upon photolysis of 6F-6F films might increase by two orders of magnitude, or more. This would make the efficiency for formation of the anhydride on the same order of magnitude as the efficiency for its decomposition in air. Thus, we would expect to see a steady-state concentration of anhydride in the photolyzed 6F-6F films, as is observed in Figure 10a and Figure 15.

Two other facts are important in the overall photodecomposition process. First, the phthalimide group, formed to a lower extent in the initial photolysis step, has a quantum efficiency for decomposition (0.047) comparable to that for phthalic anhydride. Also, nitrosobenzene (assuming that it is formed) and subsequently formed nitrobenzene, are readily photooxidized. In addition, one of the primary photooxidation products of phthalic anhydride is benzoic acid which would rapidly oxidize by decarboxylation under aerobic photolysis conditions. Thus, all of the primary and secondary photoproducts, once formed, rapidly photooxidize to give small molecule products such as carbon dioxide, carbon monoxide, etc., provided that the proper wavelength of light is employed.

In a previous paper we demonstrated that phthalic anhydride, nitrobenzene, and phthalimide end groups require exposure to light of wavelength less than about 300 nm to effect rapid photooxidative decomposition. Therefore, even though light of wavelength greater than 300 nm can induce chain cleavage via photooxidation of the basic phthalimide chromophore, in order to complete the rapid photooxidative ablation process wavelengths of light less than 300 nm, such as are obtained with an unfiltered medium pressure mercury lamp, are required. This is true even for the photolabile 6F-6F polyimide.

## CONCLUSIONS

In this paper, we have shown the effect of solvent polarity and electron withdrawing and electron accepting groups on the photochemistry/photophysics of N-arylphthalimides. Electron withdrawing groups at the para position of the N-phenyl ring enhance the photooxidation process and phthalic anhydride formation by two orders of magnitude compared to electron withdrawing groups substituted at the same position. An increase in the same direction is found for the relative yield of triplet state. The implication of the small molecule model study for polyimides with reduced charge-transfer character is that electron withdrawing groups substituted at the para position of the N-phenyl unit should result in enhanced photolability. Indeed, this is the case for the highly photooxidatively unstable 6F-6F polyimides. Complete photooxidation of this 6F-6F films can be accomplished in a matter of a few hours with an unfiltered medium pressure mercury

lamp. In addition, the ablation is a very clean process leading to no surface pitting which often occurs when polyimides are ablatively etched with a laser. Apparently, anhydride groups formed on the surface, which have been identified in this study by difference IR spectroscopy, are subsequently photooxidized in a series of steps to produce carbon monoxide, carbon dioxide, water, and small molecule fluorocarbons.

Despite our success in elucidating the steps in the sequential photooxidative degradation of 6F-ODA and 6F-6F films, several critical questions remain to be answered. Future papers will address the spin multiplicity of the excited state leading to the initial photochemical process, which may be an N-CO  $\alpha$ -cleavage (see reference 5) to generate a diradical which can be intercepted by oxygen (see previous paper in this series for a description of this possibility). In addition, the possibility of wavelength dependent photochemistry (and photophysics) has yet to be addressed. Since a charge-transfer state, which can be directly populated by excitation of N-arylphthalimide at wavelengths well above 300 nm, might well lead to a different or modified yield of certain products, the possibility of wavelength dependent photochemistry requires investigation.

Finally, we conclude by noting that although the processes may not be directly related, the present work may well have implications for laser-induced etching of polyimides. It may well be that the extent of charge-transfer in the excited state affects the laser ablation process as it does the photooxidation induced by an unfiltered medium pressure mercury lamp.

## ACKNOWLEDGEMENT

The authors acknowledge the financial support of the Office of Naval Research. This work was also supported, in part, by the National Science Foundation (RII-8902064), the State of Mississippi, and the University of Southern Mississippi.

## REFERENCES

1. Hoyle, C.E. and Anzures, E.T. *J. Appl. Polym. Sci.*, **1991**, 43, 1, 1.
2. Hoyle, C.E. and Anzures, E.T. *J. Appl. Polym. Sci.*, **1991**, 43, 1.
3. Anzures, E.T. and Hoyle, C.E. *Polymer Preprints*, **1990**, 31, 343.
4. Hoyle, C.E. and Anzures, E.T. paper III in series, submitted for publication in *J. Polym. Sci. Chem. Ed.*.
5. Hoyle, C.E. and Anzures, E.T., paper IV in series, submitted for publication in *Polymer*.
6. Ishida, H.; Wellinghoff, S.T.; Baer, E.; Koenig, J.L. *Macromolecules* **1980**, 13, 826.
7. LaFemina, J.P.; Arjavalingham, G.; Hougham, G. *J. Chem. Phys.* **1989**, 90, 5154.
8. LaFemina, J.P.; Arjavalingham, G.; Hougham, G. In *Polyimides: Materials, Chemistry and Characterization*; Feger, C.; Khojasteh, M.M.; McGrath, J.E., Eds.; Elsevier: New York, **1989**; p. 625.
9. Arjavalingham, G.; Hougham, G.; LaFemina, J.P. *Polymer*, **1990**, 31, 840.
10. Wachsman, E.D.; Martin, P.S.; Frank, C.W. in *Polymeric Materials for Electronics Packaging and Interconnection*; ACS Symposium Series 407; Lupinski, J.H.; Moore, R.S., Eds.; American Chemical Society, Washington, D.C., **1989**; p. 26.
11. Martin, P.S.; Wachsman, E.D.; Frank, C.W. In *Polyimides: Materials, Chemistry and Characterization*; Feger, C.; Khojasteh, M.M.; McGrath, J.E. Eds.; Elsevier: New York, **1989**; p. 371.
12. Wachsman, E.D.; Frank, C.W. *Polymer*, **1988**, 29, 1191.

13. Hayashi, R.; Tazuke, S.; Frank, C. *Macromolecules*, 1987, 20, 983.

Table I				
Solvent	$\Phi_{\text{loss}}$	$\Phi_{\text{PhAnh}}$	Relative <sup>a</sup> Triplet Yield	Fluorescence $\lambda_{\text{max}}$
Acetonitrile	$6.3 \times 10^{-4}$	$2.8 \times 10^{-4}$	0.3	525 nm
Dichloromethane	$8.2 \times 10^{-4}$	$3.2 \times 10^{-4}$	0.21	520 nm
Cyclohexane	$9.3 \times 10^{-3}$	$5.0 \times 10^{-3}$	1.0	490 nm

<sup>a</sup>Values subject to  $\pm 20\%$  error due to some variation in absorbance at excitation wavelength as well as possible differences in extinction coefficients at peak maxima: also, values not corrected for variation in laser pulse power.

Compound	$\lambda_{\max}^a$ (Fluorescence)	$\Phi_{\text{loss}}^b$	$\Phi_{\text{PhAnh}}^b$	Relative Triplet Yield <sup>d</sup>
PA-A	520 (538)	$8.2 \times 10^{-4}$	$5.2 \times 10^{-4}$	1.0
PA-POA	550 (too weak)	$8.8 \times 10^{-5}$	<sup>c</sup> $1.4 \times 10^{-4}$	0.5
PA-CIA	525 (546)	$8.3 \times 10^{-4}$	$2.8 \times 10^{-4}$	Not determined
PA-CNA	470 (513)	$1.3 \times 10^{-2}$	$5.5 \times 10^{-3}$	8.9

<sup>a</sup>Determined in cyclohexane.  $\lambda_{\text{ex}} = 325$  nm. Similar trend noted (in parentheses) when determined in dichloromethane, except maxima are shifted and lower in intensity.

<sup>b</sup>Except where noted, determined in dichloromethane.  $\lambda_{\text{ex}} = 313$  nm.

<sup>c</sup>Determined in acetonitrile.  $\lambda_{\text{ex}} = 313$  nm.

<sup>d</sup>Determined in dichloromethane.  $\lambda_{\text{ex}} = 248$  nm. Values subject to  $\pm 20\%$  error due to some variation in absorbance at excitation wavelength as well as possible differences in extinction coefficients at peak maxima: also values not corrected for variation in laser pulse power.

## FIGURE CAPTIONS

- Figure 1. Absorption spectra of PA-A in several solvents (a)  $3.6 \times 10^{-4}$  M in cyclohexane; (b)  $3.7 \times 10^{-4}$  M in  $\text{CH}_2\text{Cl}_2$ ; (c)  $3.8 \times 10^{-4}$  M in  $\text{CH}_3\text{CN}$ .
- Figure 2. Fluorescence spectra ( $\lambda_{\text{ex}} = 325$  nm) of PA-A in several solvents. (a)  $1.49 \times 10^{-3}$  M in cyclohexane; (b)  $1.51 \times 10^{-3}$  M in  $\text{CH}_2\text{Cl}_2$ ; (c)  $1.54 \times 10^{-3}$  M in  $\text{CH}_3\text{CN}$ .
- Figure 3. Transient absorption spectra of N-phenylphthalimide in methylene chloride at different time intervals after the flash, (a) air saturated, and (b) nitrogen saturated.
- Figure 4. Transient absorption spectra of N-phenylphthalimide in acetonitrile at different time intervals after the flash, (a) air saturated, and (b) nitrogen saturated.
- Figure 5. Transient absorption spectra of N-phenylphthalimide in cyclohexane at different time intervals after the flash, (a) air saturated, and (b) nitrogen saturated.
- Figure 6. Stern-Volmer plot for the quenching of N-phenylphthalimide transient by 1,3-cyclohexadiene.
- Figure 7. Absorption spectra of N-aryl phthalimide model compounds in cyclohexane. (a)  $1.56 \times 10^{-5}$  M, PA-A; (b)  $1.54 \times 10^{-5}$  M, PA-CIA (c)  $1.45 \times 10^{-4}$  M, PA-CNA; (d)  $1.52 \times 10^{-5}$  M, PA-POA

- Figure 8. Fluorescence spectra ( $\lambda_{\text{ex}} = 325 \text{ nm}$ ) of N-arylphthalimide model compounds in cyclohexane (a)  $1.56 \times 10^{-4} \text{ M}$ , PA-A; (b)  $1.54 \times 10^{-5} \text{ M}$ , PA-CIA (c)  $1.45 \times 10^{-4} \text{ M}$ , PA-CNA; (d)  $1.52 \times 10^{-5} \text{ M}$ , PA-POA.
- Figure 9. Absorption spectra of thin polyimide films on quartz slide.
- Figure 10. (a) IR spectra of 6F-6F film before and after exposure to the unfiltered medium pressure mercury lamp in air for 3 hours; (b) IR spectra of 6F-ODA film before and after exposure to the unfiltered medium pressure mercury lamp in air for 12 hours.
- Figure 11. IR spectra of 6F-6F film before (a) and after (b) exposure to the unfiltered medium pressure mercury lamp in nitrogen atmosphere for 96 hours.
- Figure 12. GPC chromatograms of 6F-6F film exposed to the unfiltered medium pressure mercury lamp in air for (a) 0h; (b) 1.0h; (c) 3.0h.
- Figure 13. Plot of molecular weight of 6F-ODA (o) and 6F-6F (★) films at peak maxima (compared to polystyrene) versus photolysis time with unfiltered medium pressure mercury lamp in air.
- Figure 14. Plot of molecular weight of 6F-ODA (o) and 6F-6F (★) films at peak maximum (compare to polystyrene) versus photolysis time with unfiltered medium pressure mercury lamp in nitrogen atmosphere.
- Figure 15. IR difference spectrum of 6F-6F film photolyzed with unfiltered medium pressure mercury lamp in air for 3 hours.

Fig. 1

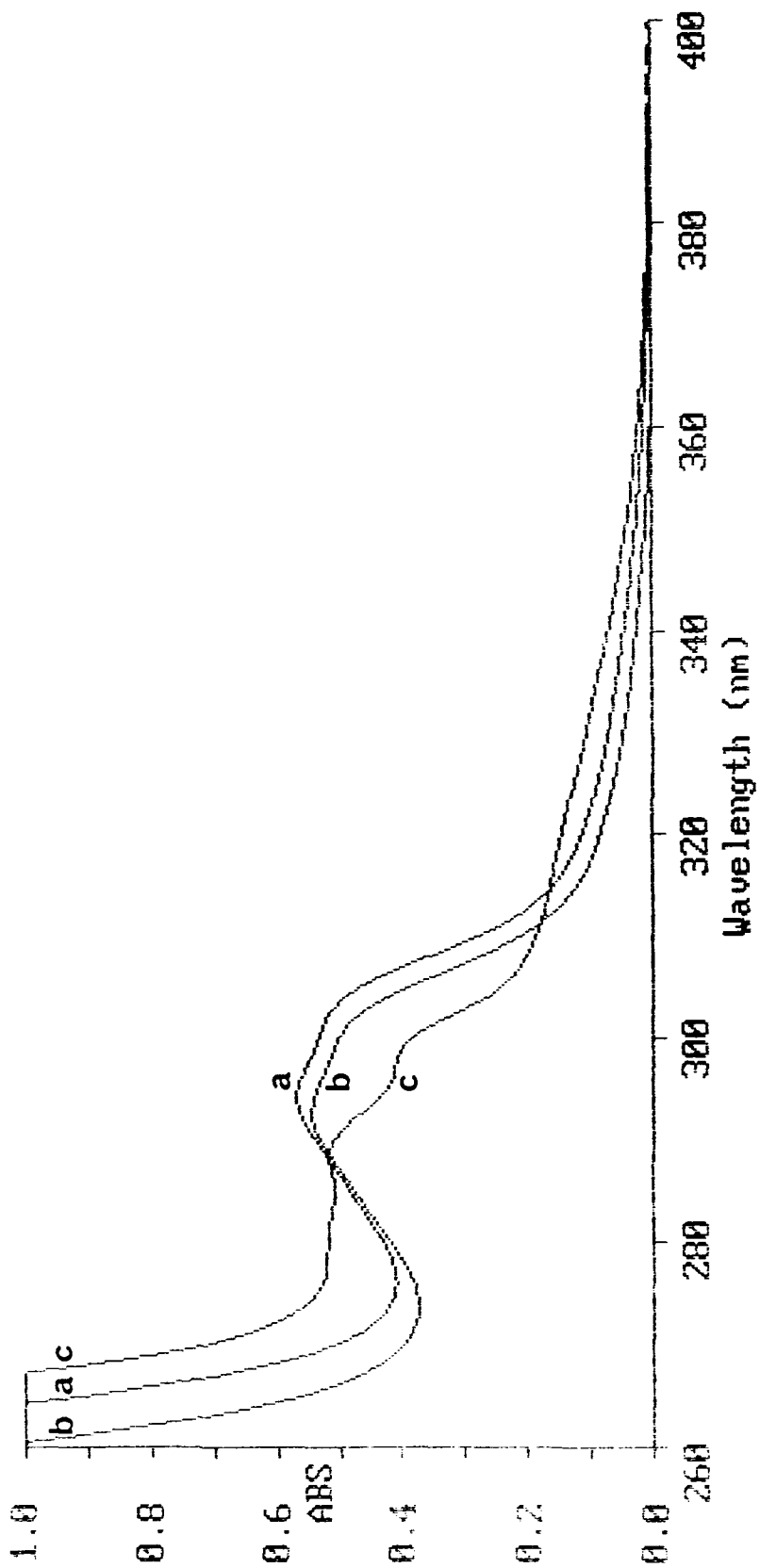


Fig. 2

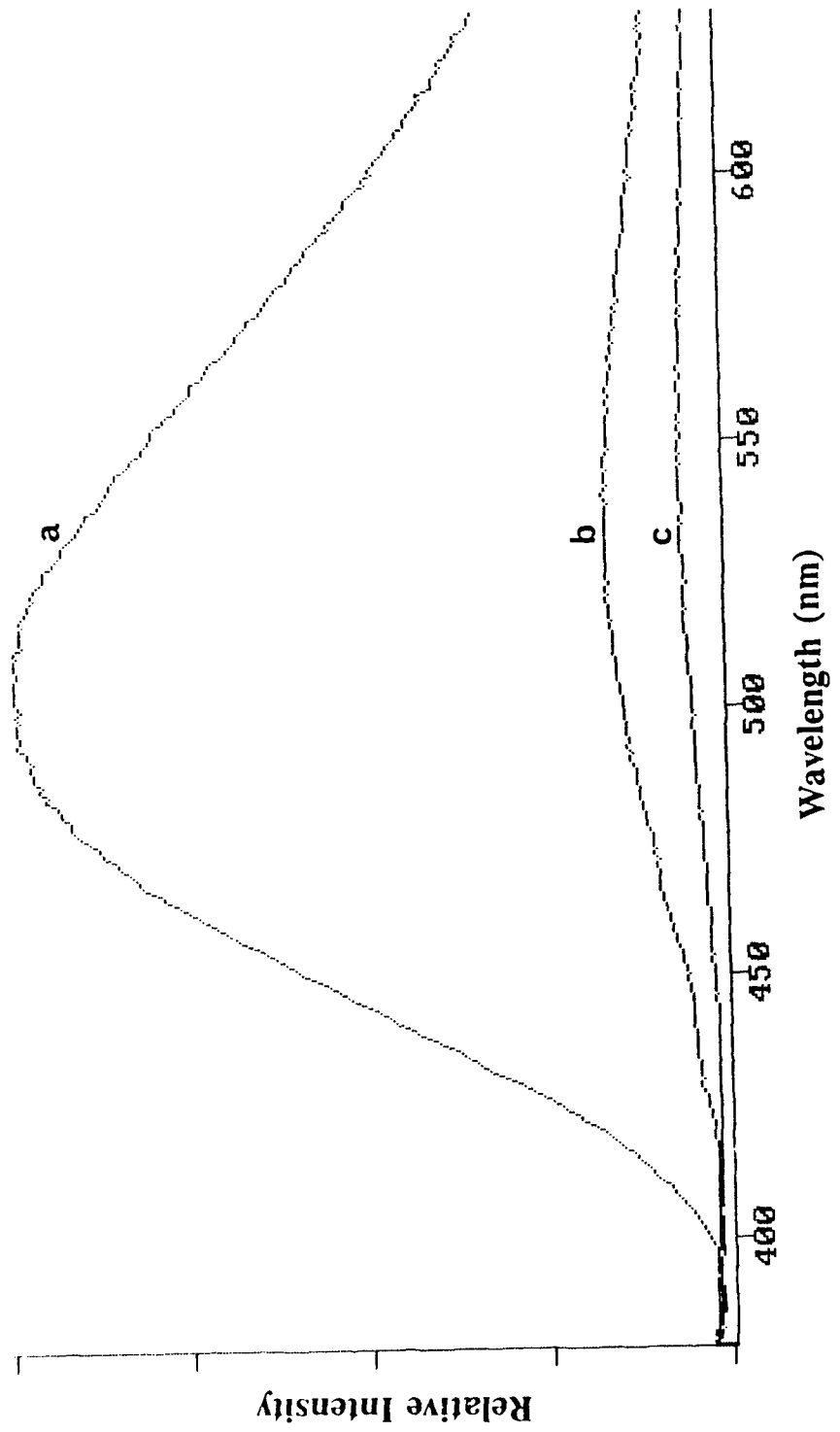


Fig. 3

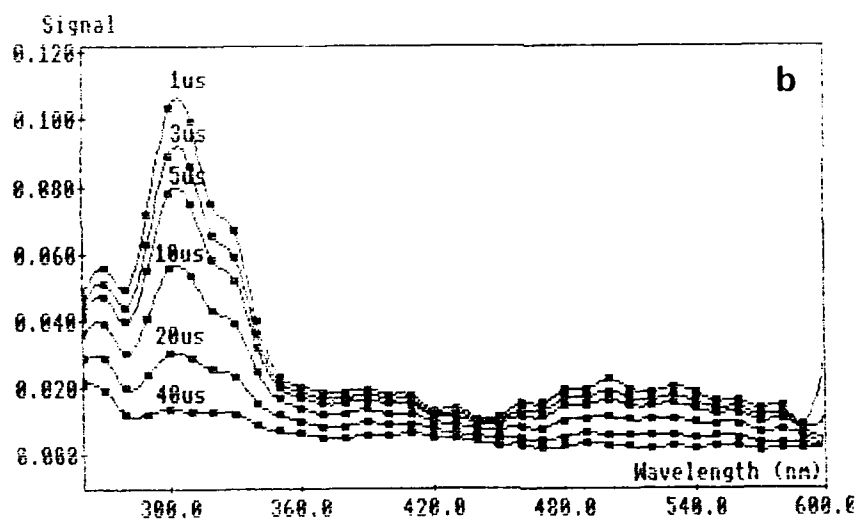
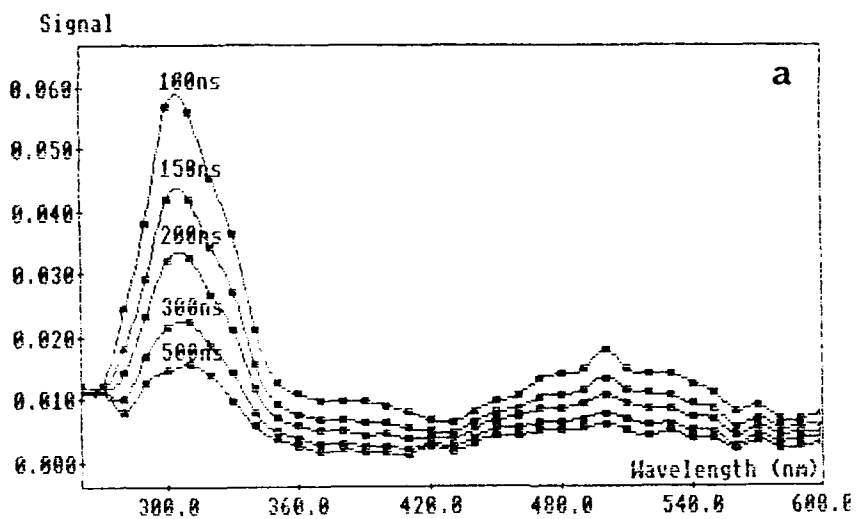


Fig. 4

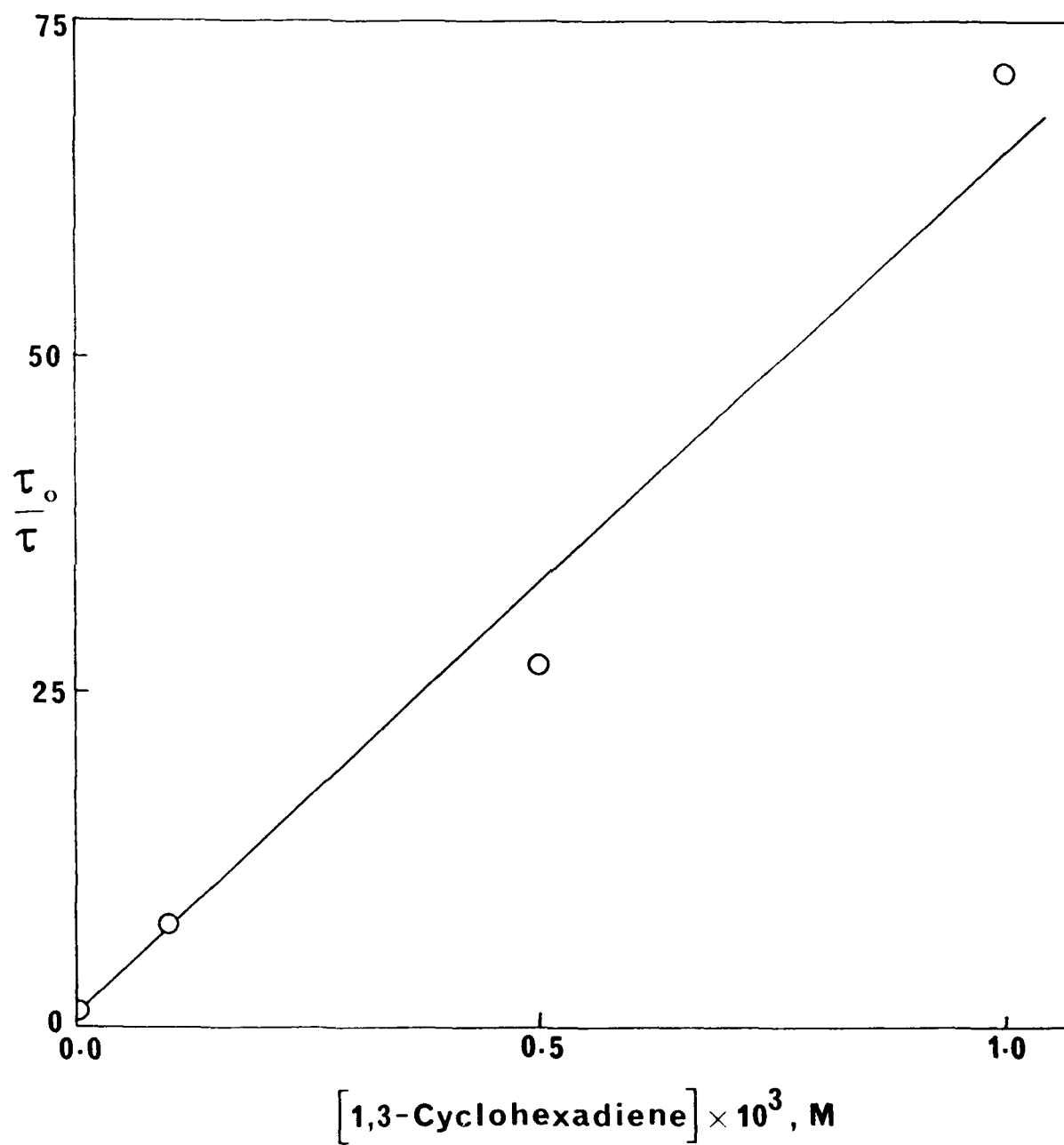


Fig. 5

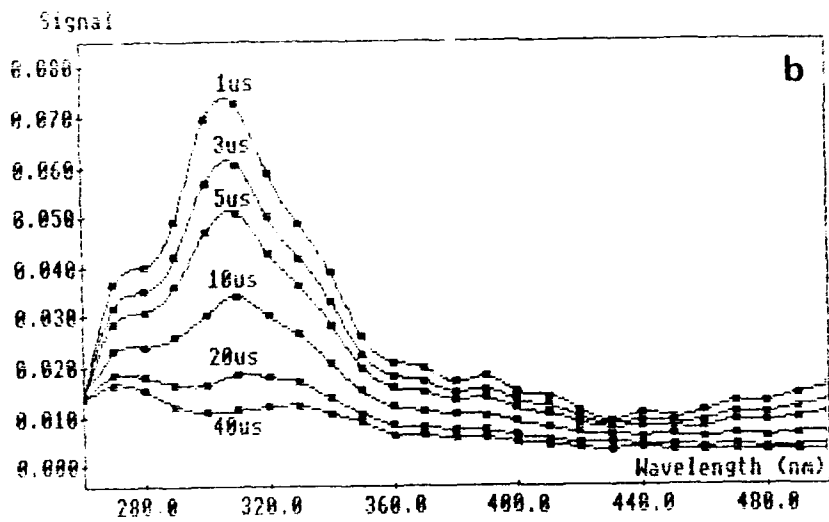
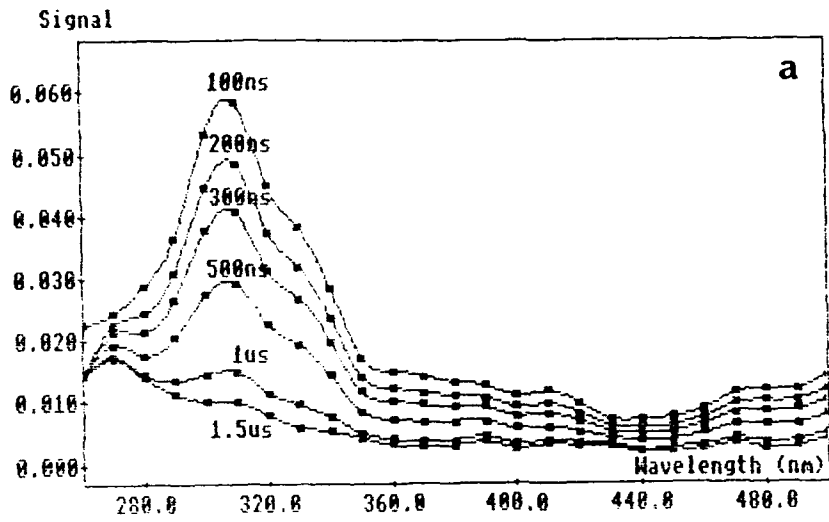




Fig. 7

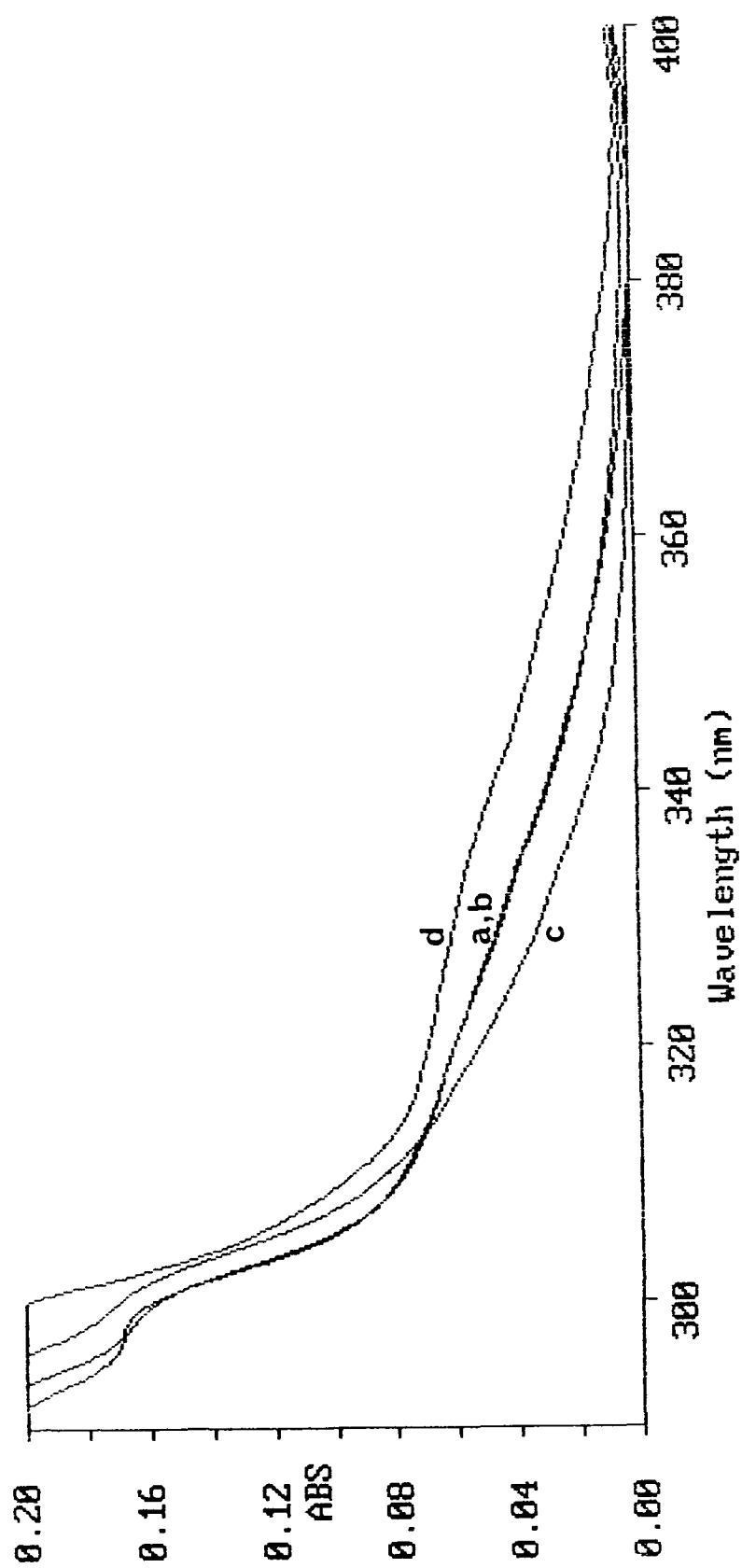


Fig. 8

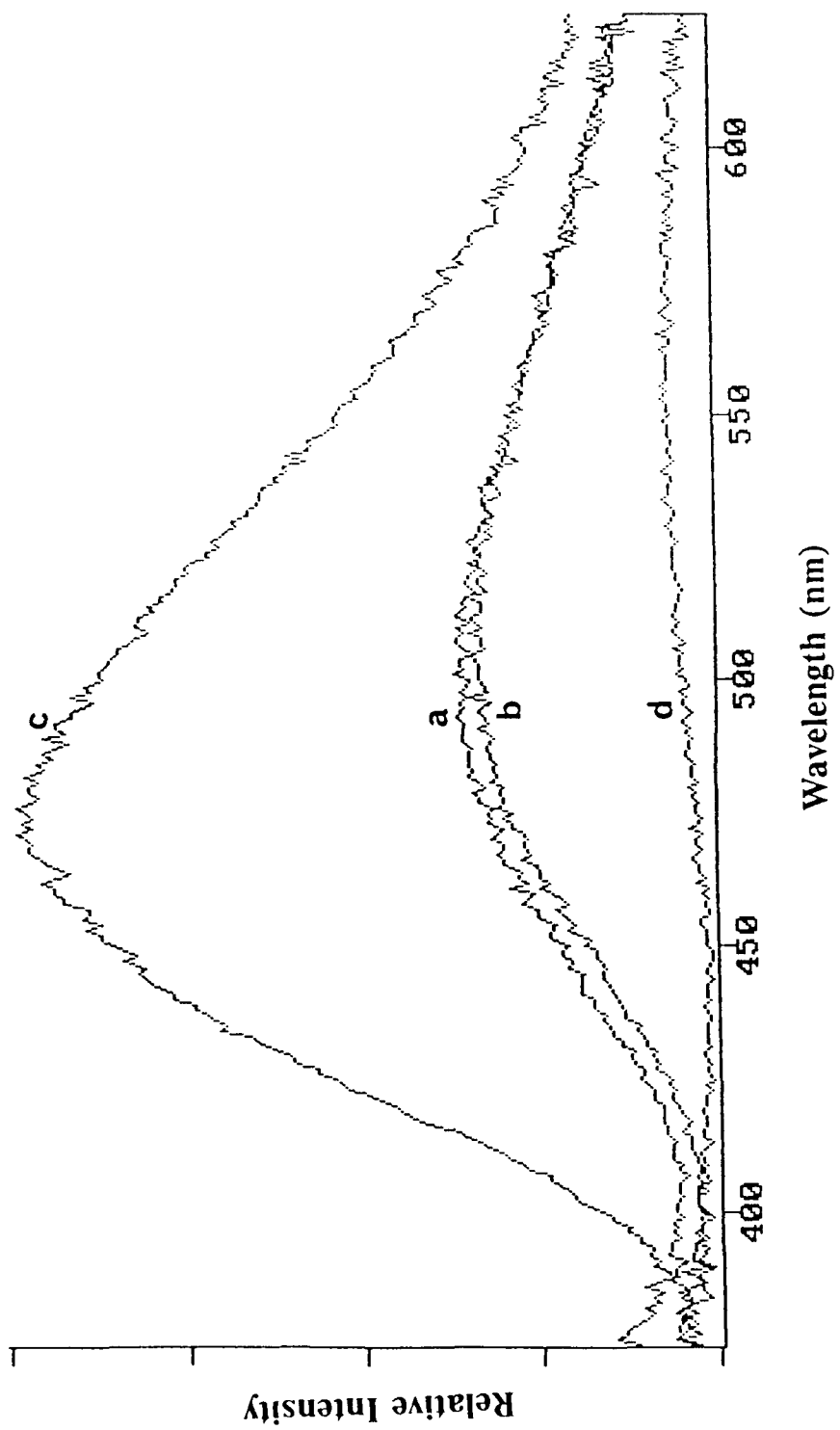


Fig. 9

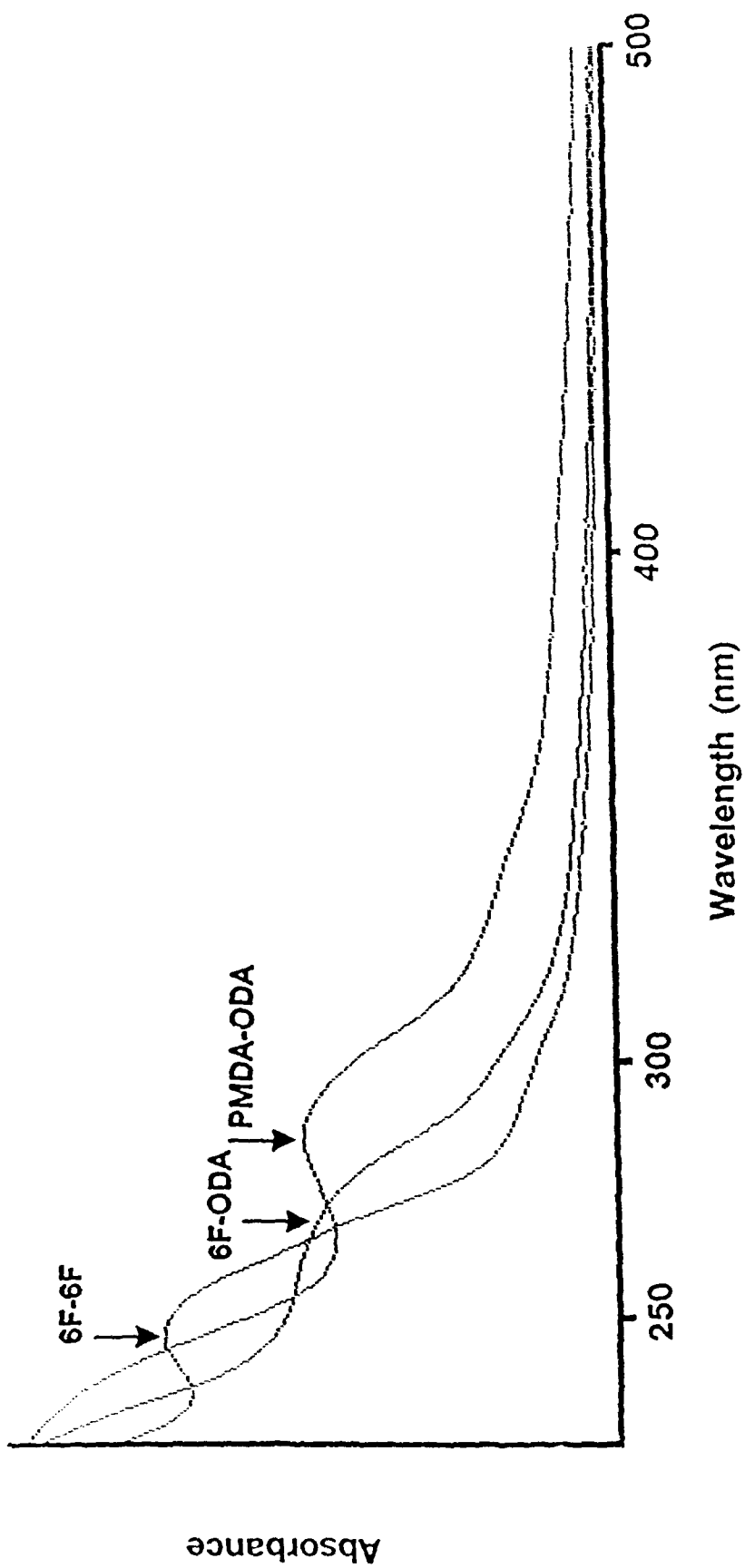


Fig. 10a

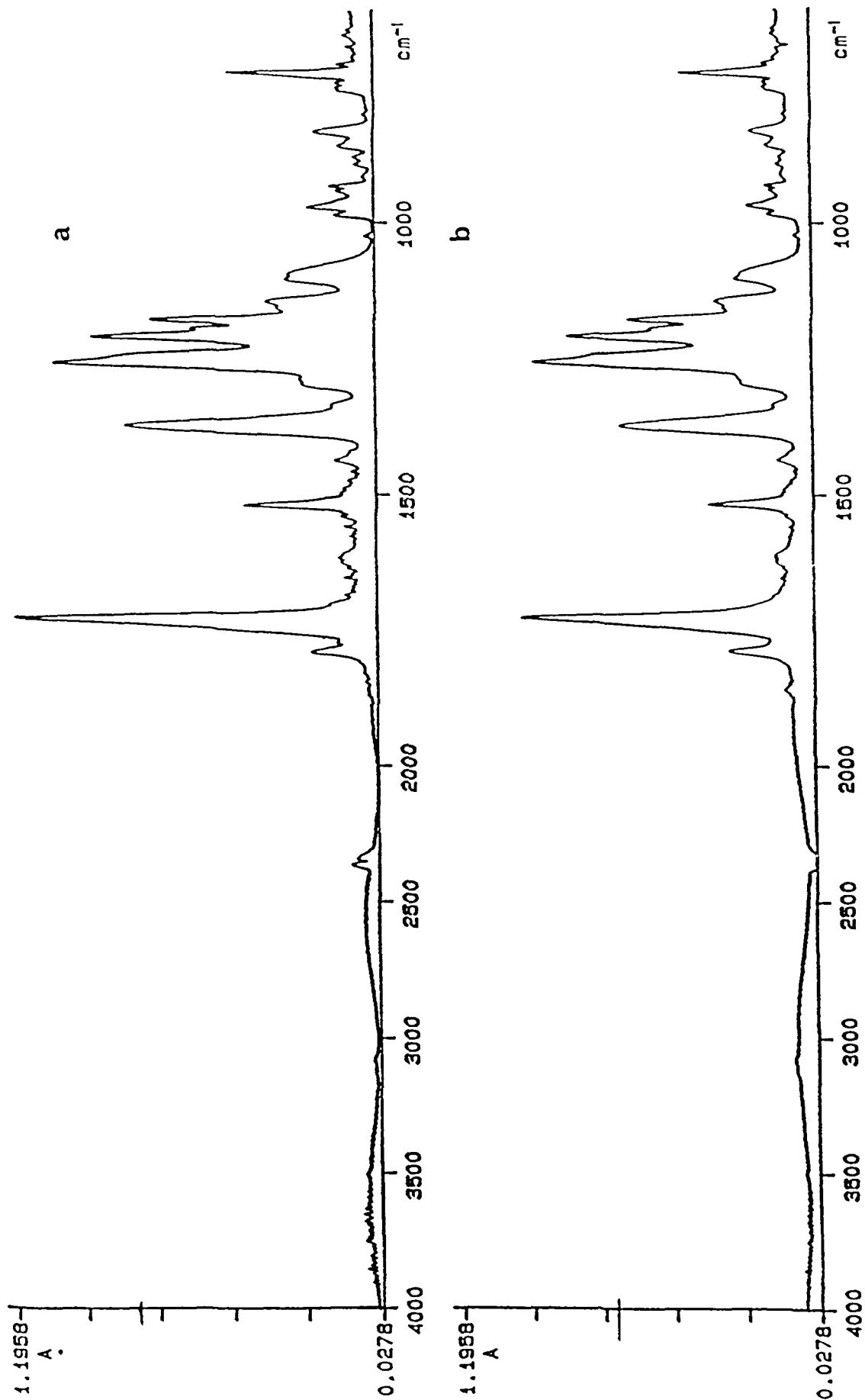


Fig. 10b

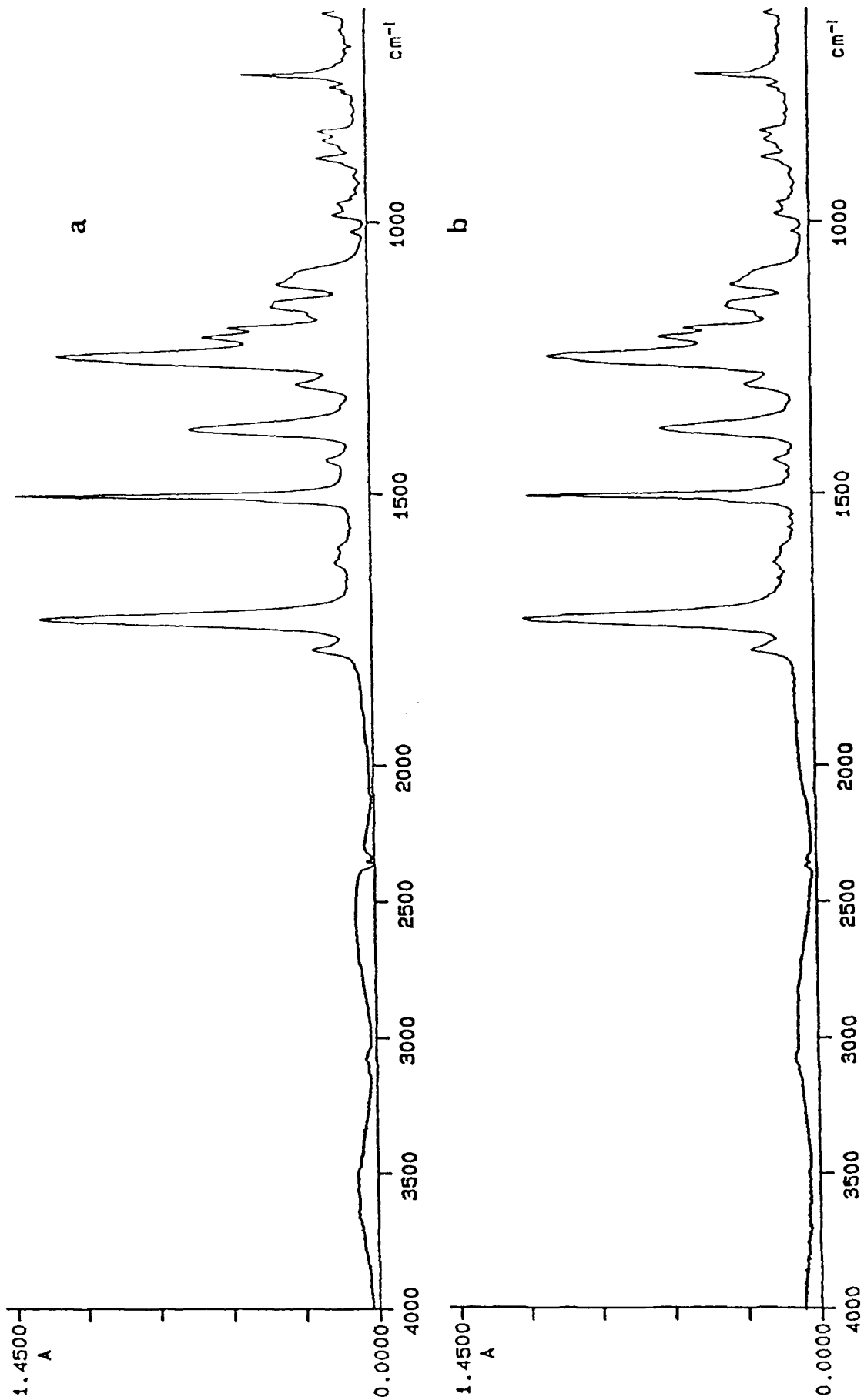


Fig. 11

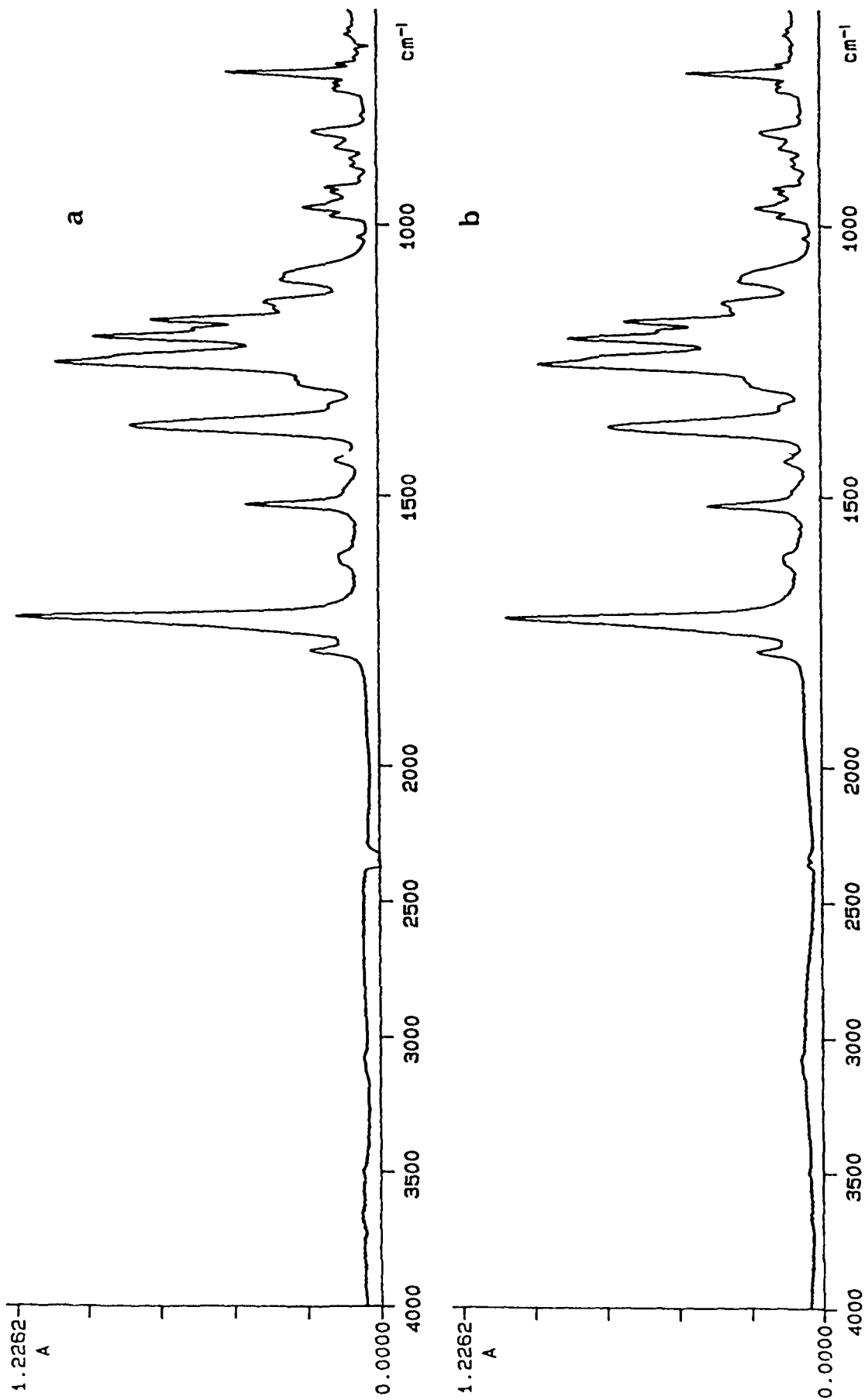


Fig. 12

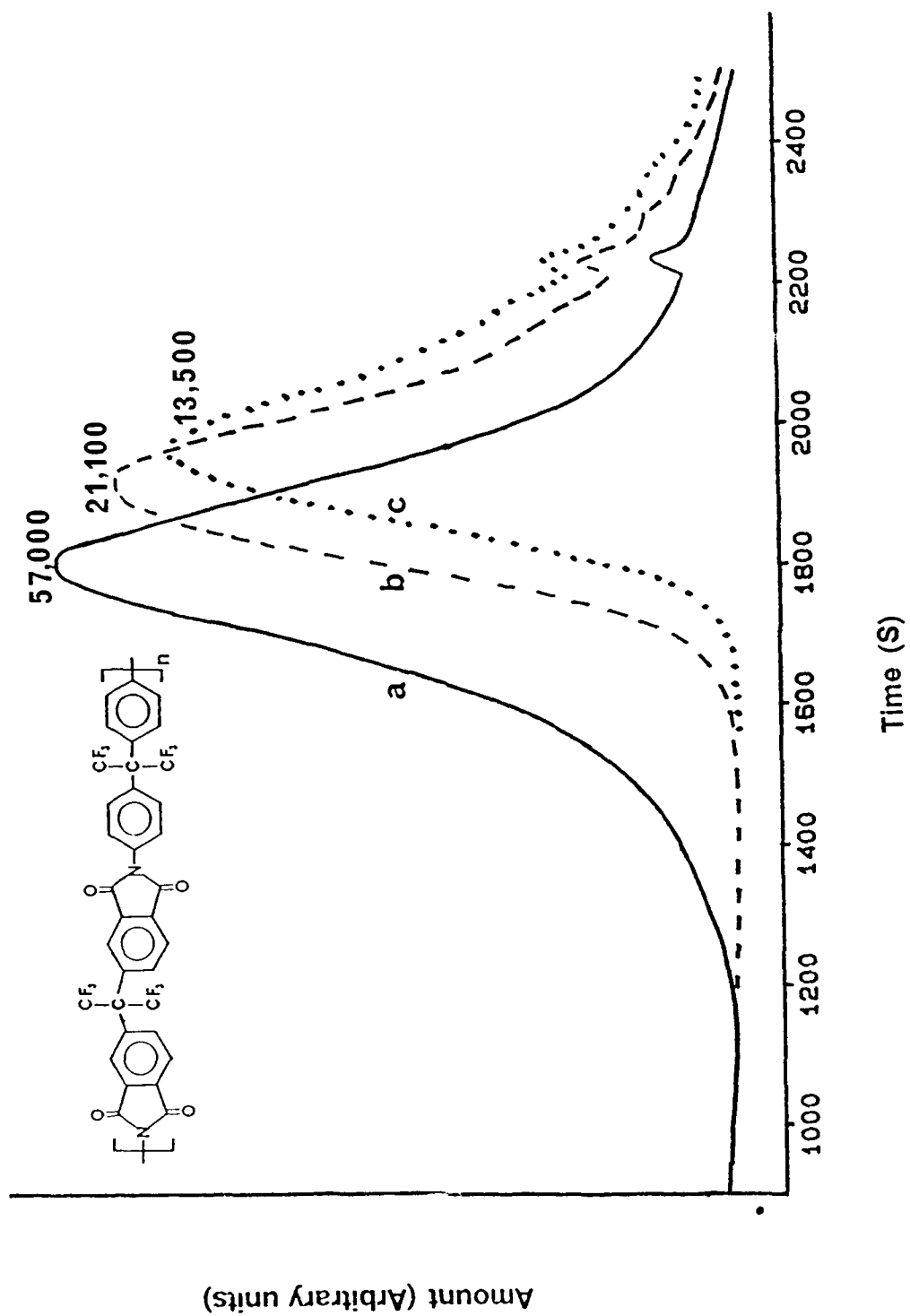


Fig. 13

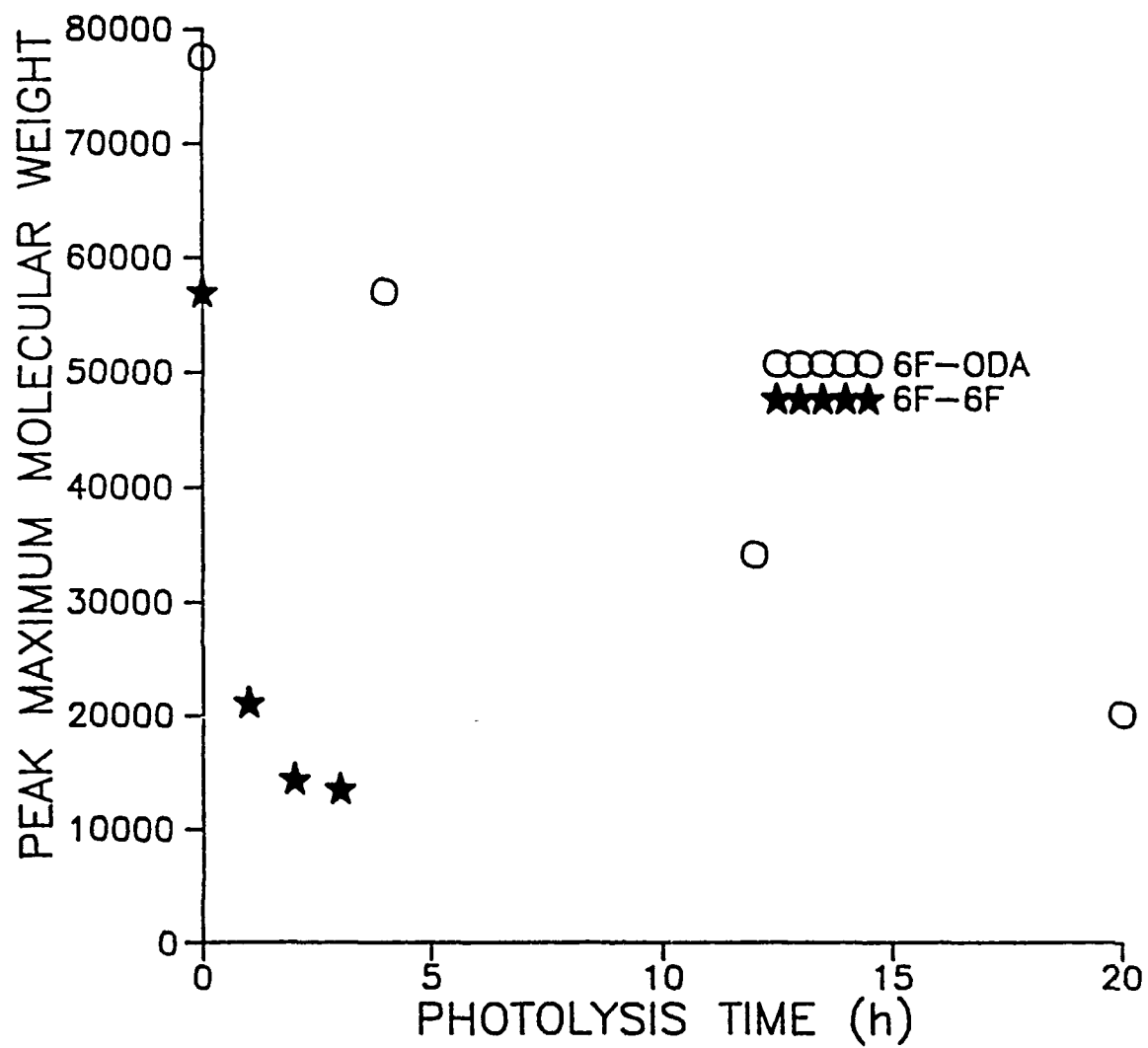


Fig. 14

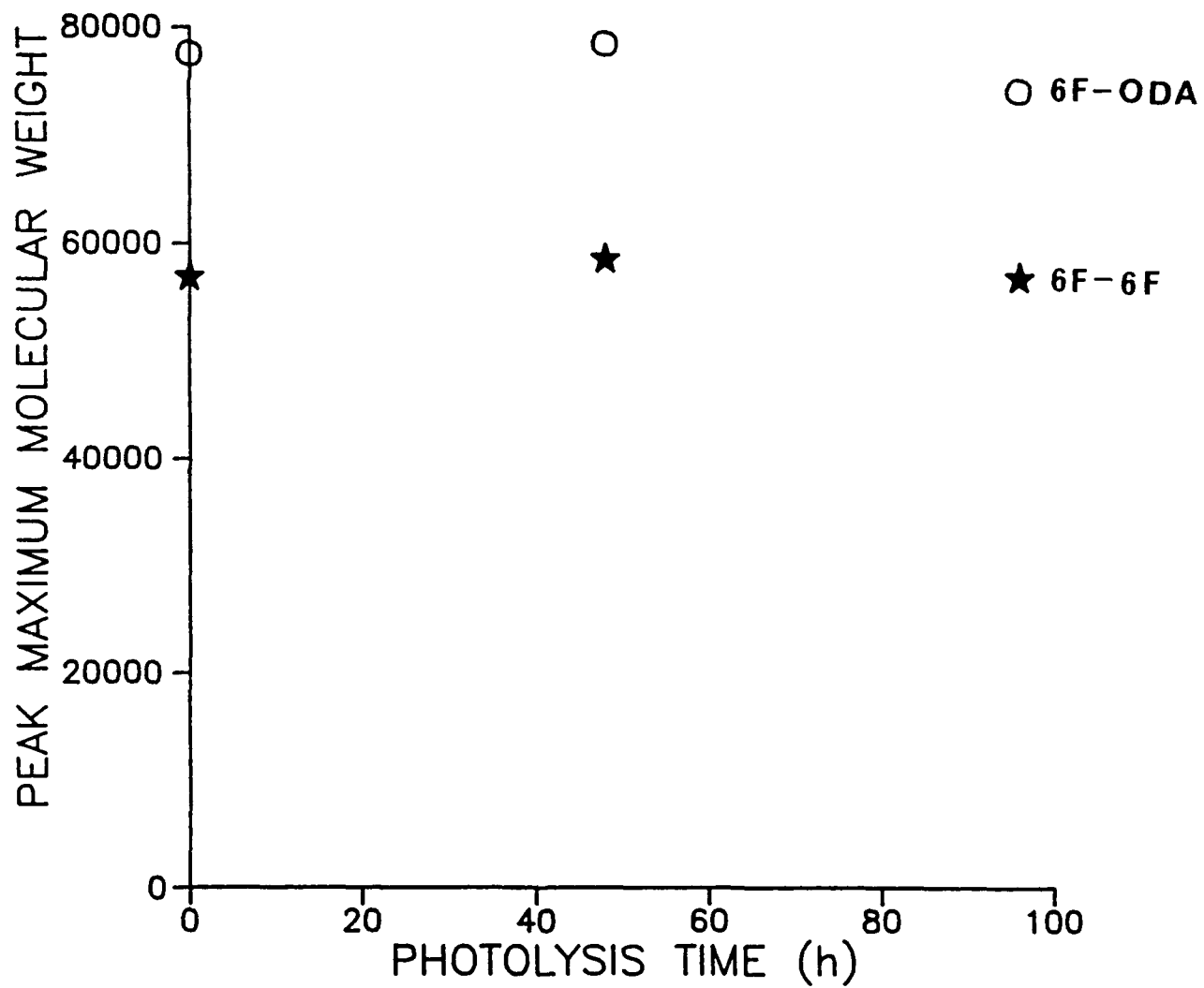


Fig. 15

